Tang et al.

Figure S1

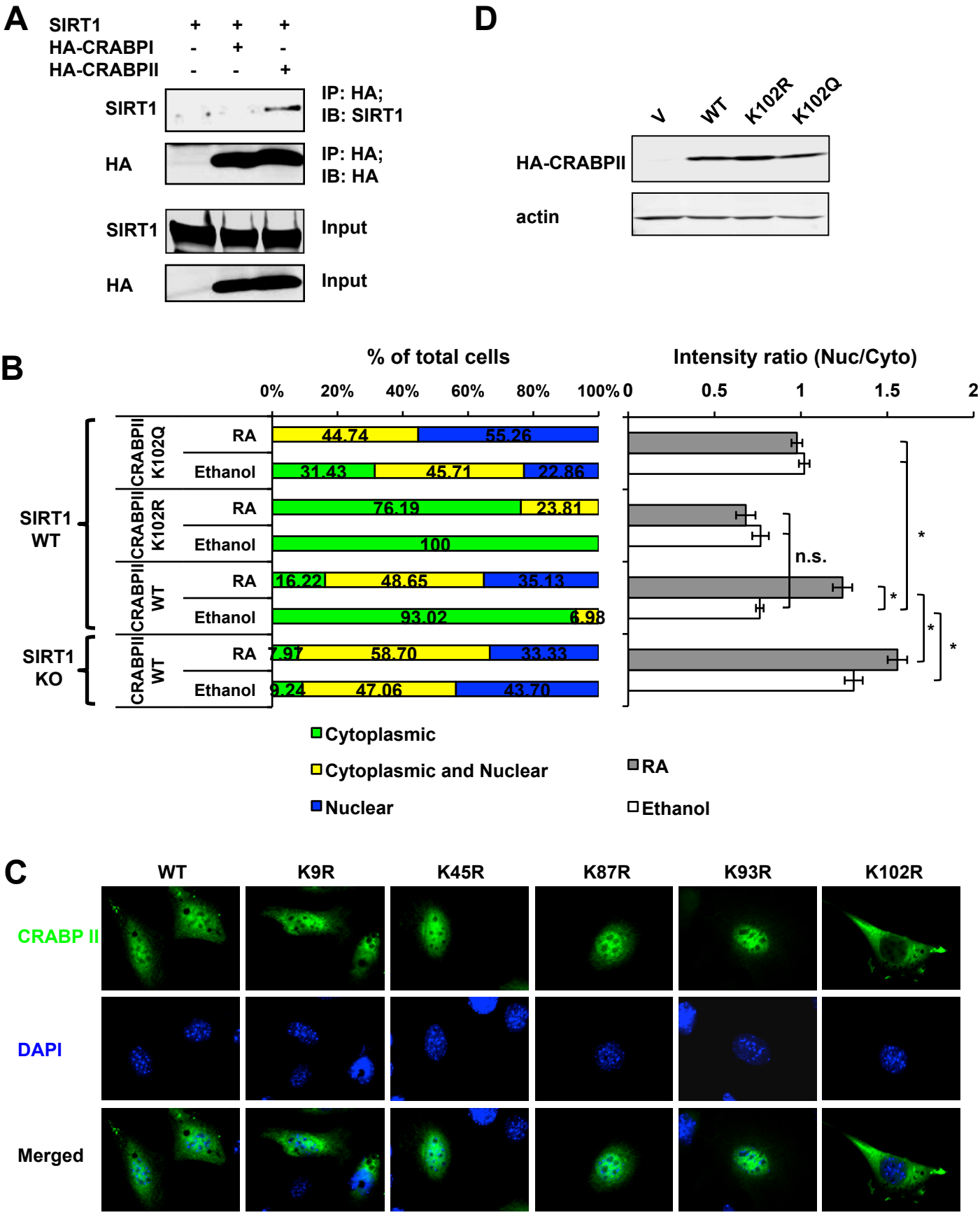

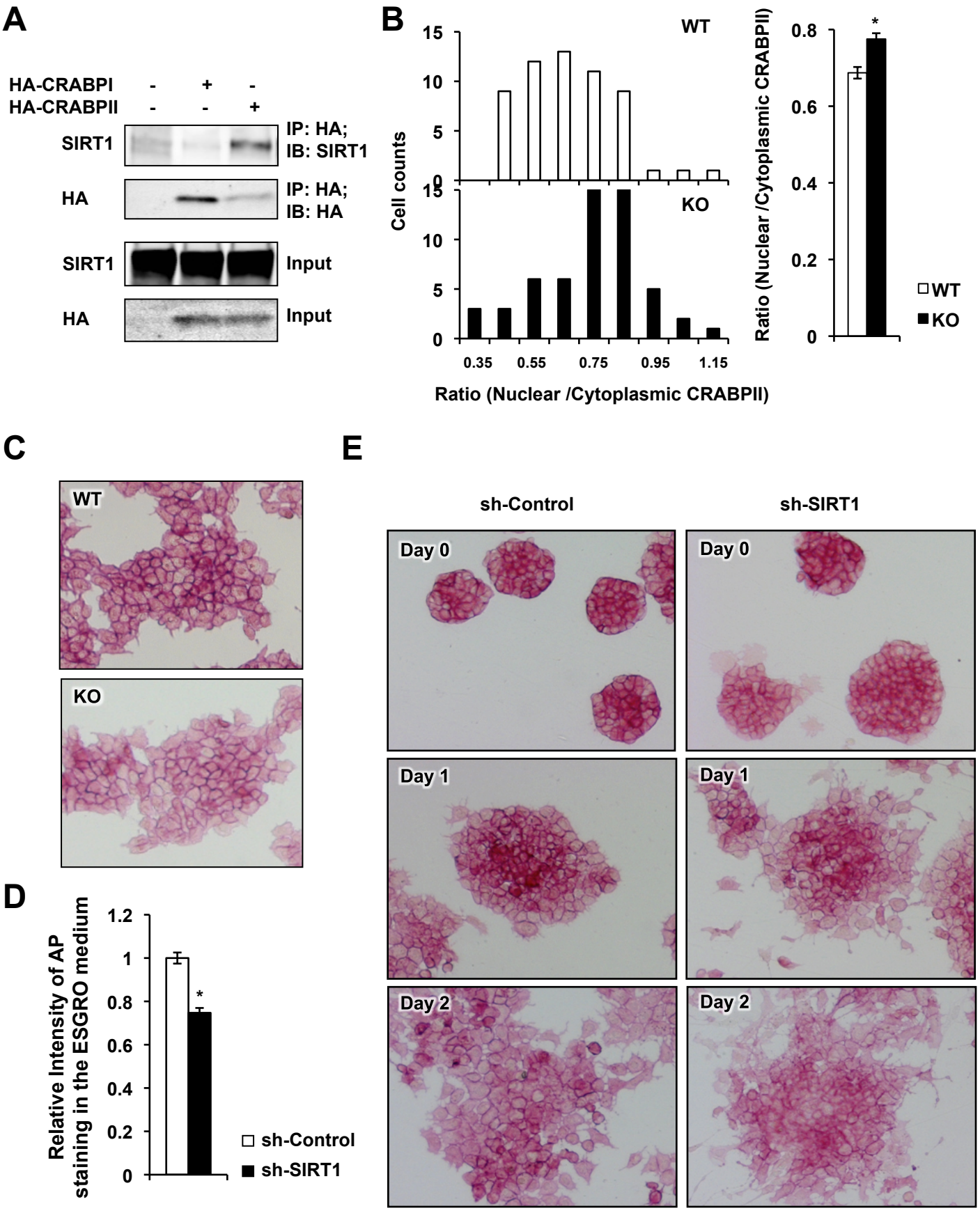
A
HA-CRABPI - + -
HA-CRABPII - - +
SIRT1
IP: HA;
IB: SIRT1
HA
IP: HA;
IB: HA
SIRT1
Input
HA
Input
B
WT
KO
Cell counts
15
10
5
0
0.35
0.55
0.75
0.95
1.15
Ratio (Nuclear /Cytoplasmic CRABPII)
Ratio (Nuclear /Cytoplasmic CRABPII)
0.8
0.6
0.4
0.2
0
*
WT
KO
C
WT
KO
D
Relative Intensity of AP staining in the ESGRO medium
1.2
1
0.8
0.6
0.4
0.2
0
*
sh-Control
sh-SIRT1
E
sh-Control
sh-SIRT1
Day 0
Day 0
Day 1
Day 1
Day 2
Day 2

A **Wnt/β-catenin signaling**

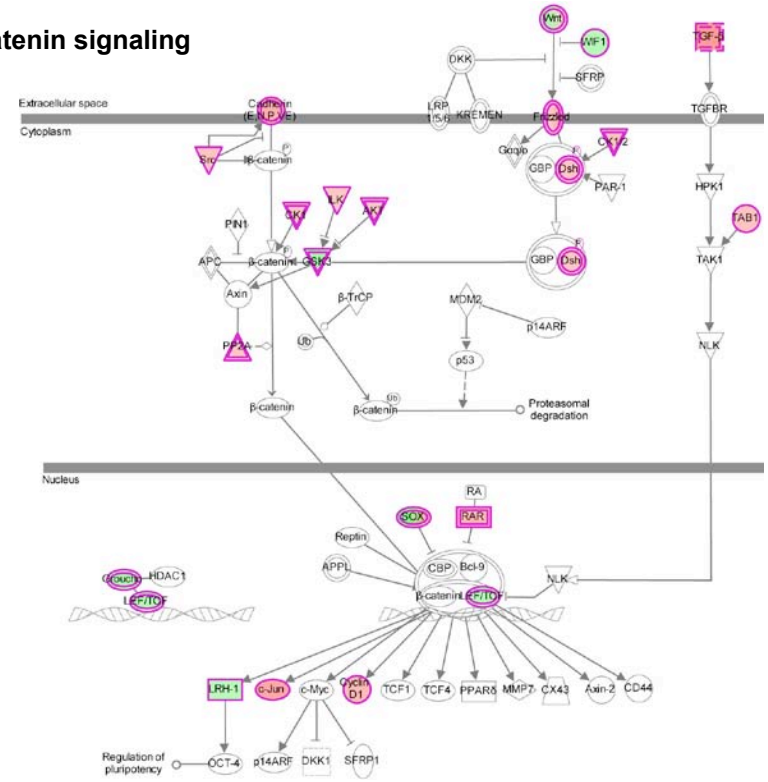

B **Role of Oct4 in Mammalian Embryonic Stem Cell Pluripotency**

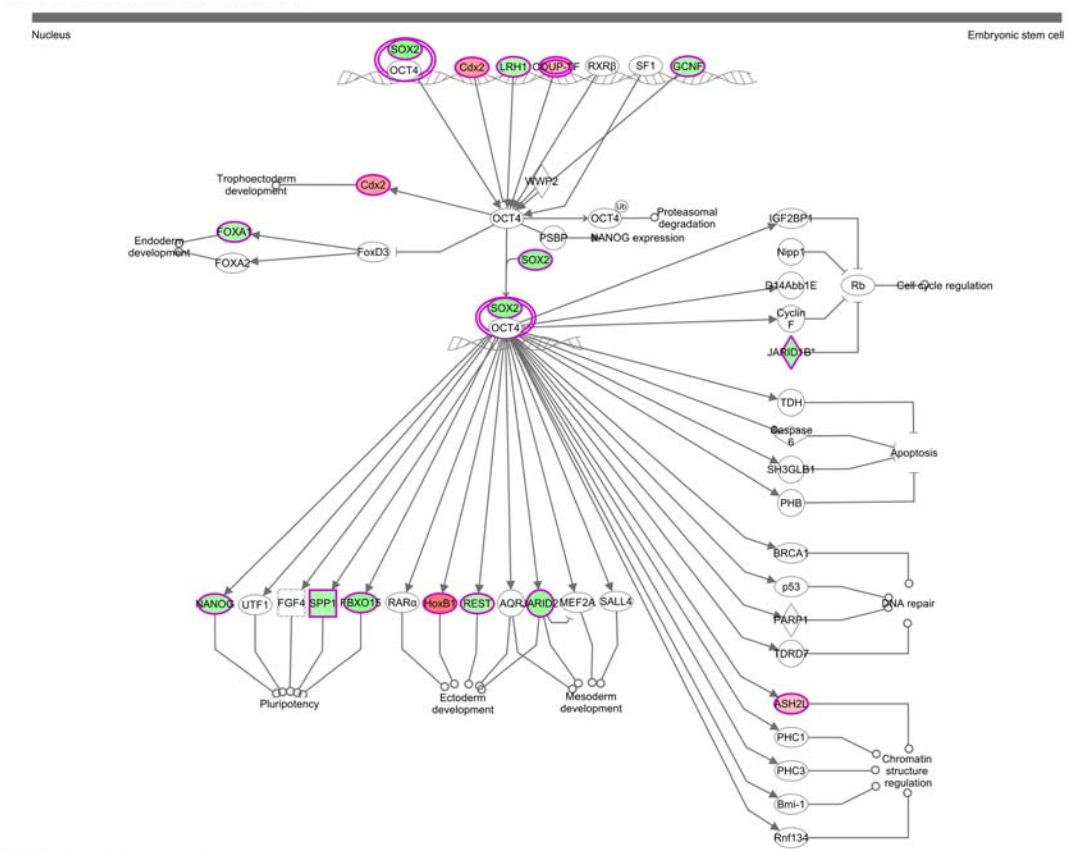

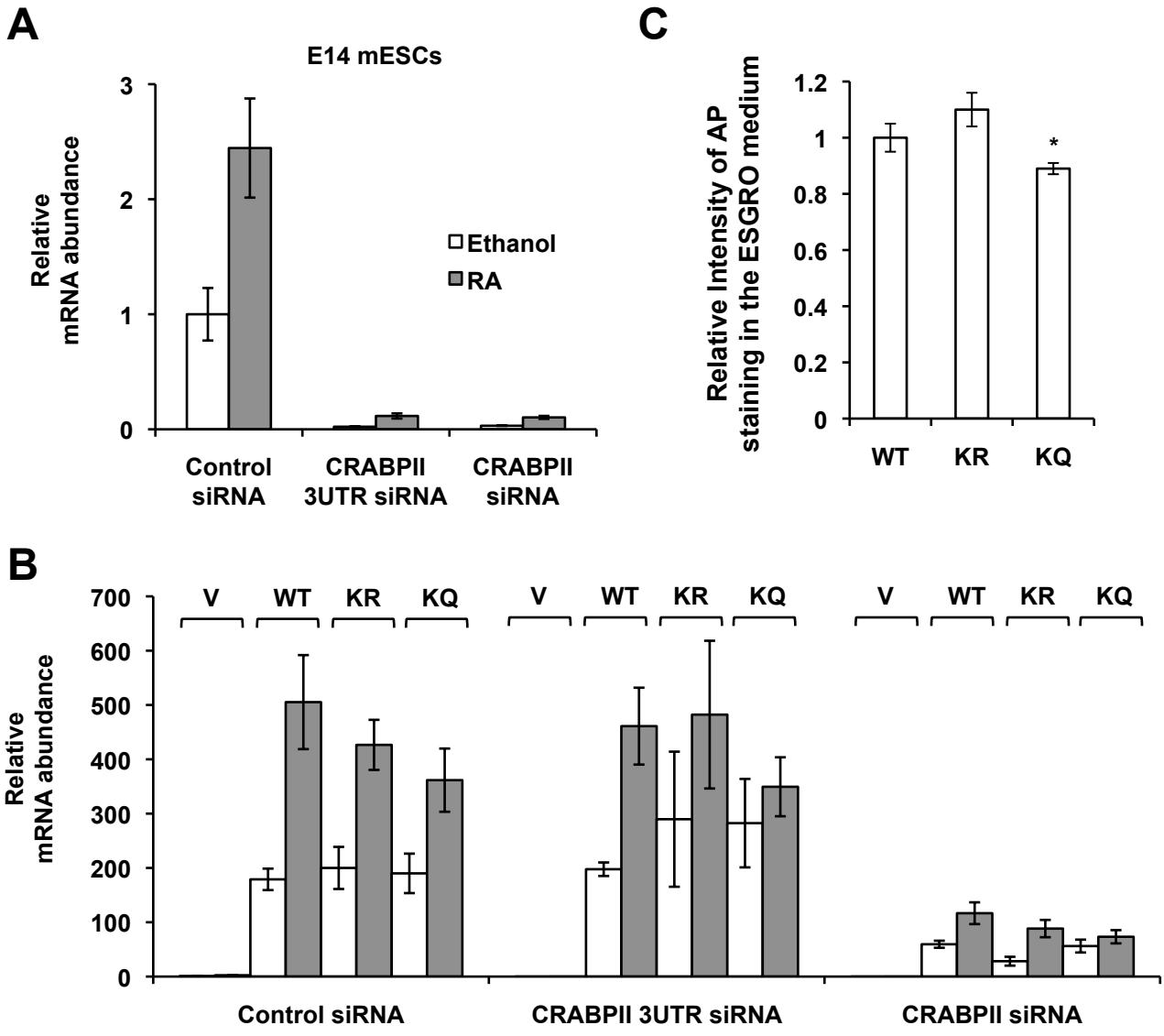
A
E14 mESCs
Relative mRNA abundance
3
2
1
0
Ethanol
RA
Control siRNA
CRABPII 3UTR siRNA
CRABPII siRNA
C
Relative Intensity of AP staining in the ESGRO medium
1.2
1
0.8
0.6
0.4
0.2
0
*
WT
KR
KQ
B
Relative mRNA abundance
700
600
500
400
300
200
100
0
V
WT
KR
KQ
Control siRNA
CRABPII 3UTR siRNA
CRABPII siRNA

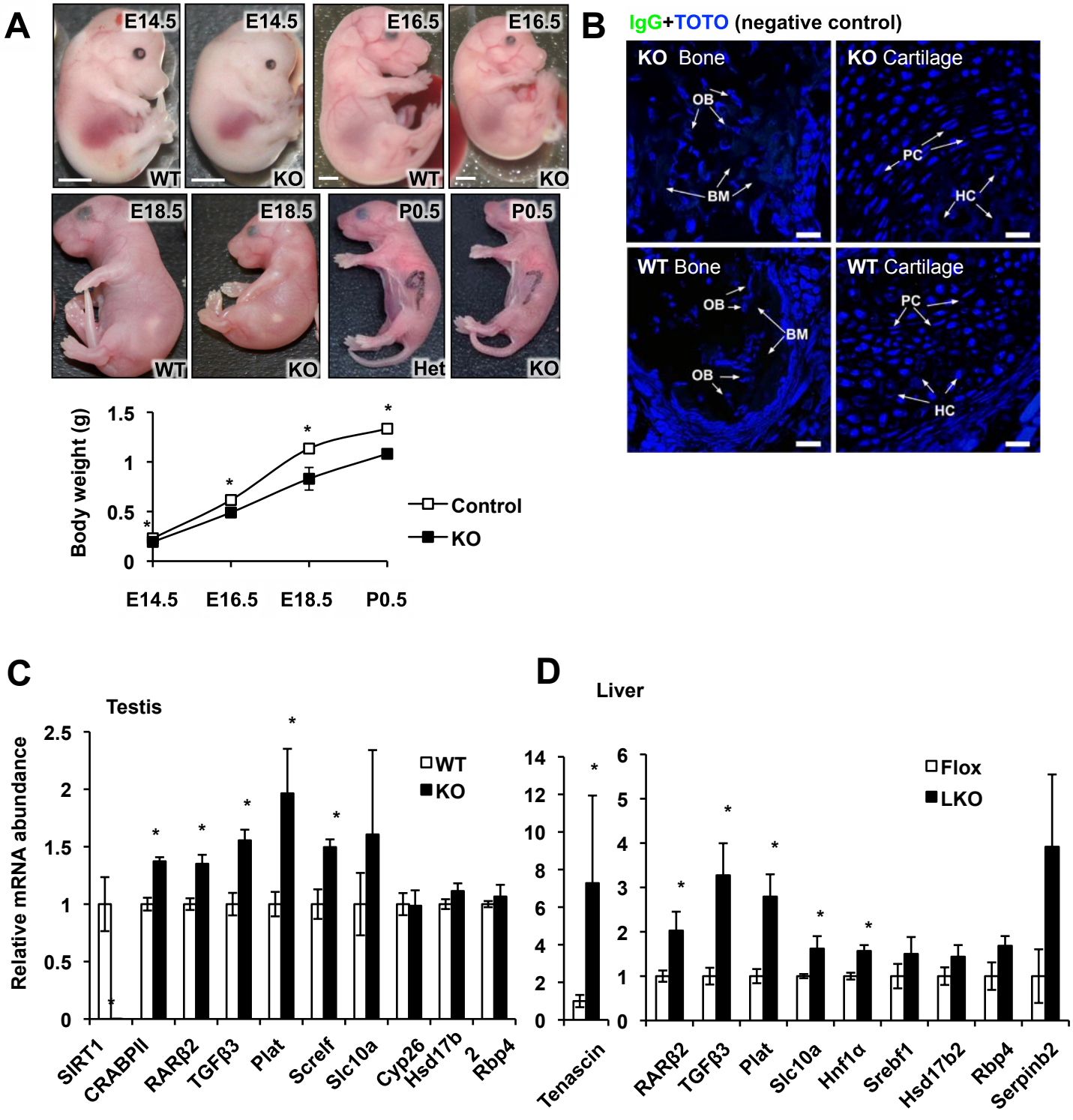
A
E14.5
WT
E14.5
KO
E16.5
WT
E16.5
KO
E18.5
WT
E18.5
KO
P0.5
Het
P0.5
KO
Body weight (g)
1.5
1
0.5
0
E14.5
E16.5
E18.5
P0.5
Control
KO
B
IgG+TOTO (negative control)
KO Bone
OB
BM
KO Cartilage
PC
HC
WT Bone
OB
BM
OB
WT Cartilage
PC
HC
C
Testis
Relative mRNA abundance
2.5
2
1.5
1
0.5
0
WT
KO
SIRT1
CRABPII
RARβ2
TGFβ3
Plat
Screlf
Slc10a
Cyp26
Hsd17b 2
Rbp4
D
Liver
14
12
10
8
6
4
2
0
6
5
3
2
1
0
Flox
LKO
Tenascin
RARβ2
TGFβ3
Plat
Slc10a
Hnf1α
Srebf1
Hsd17b2
Rbp4
Serpinb2

A

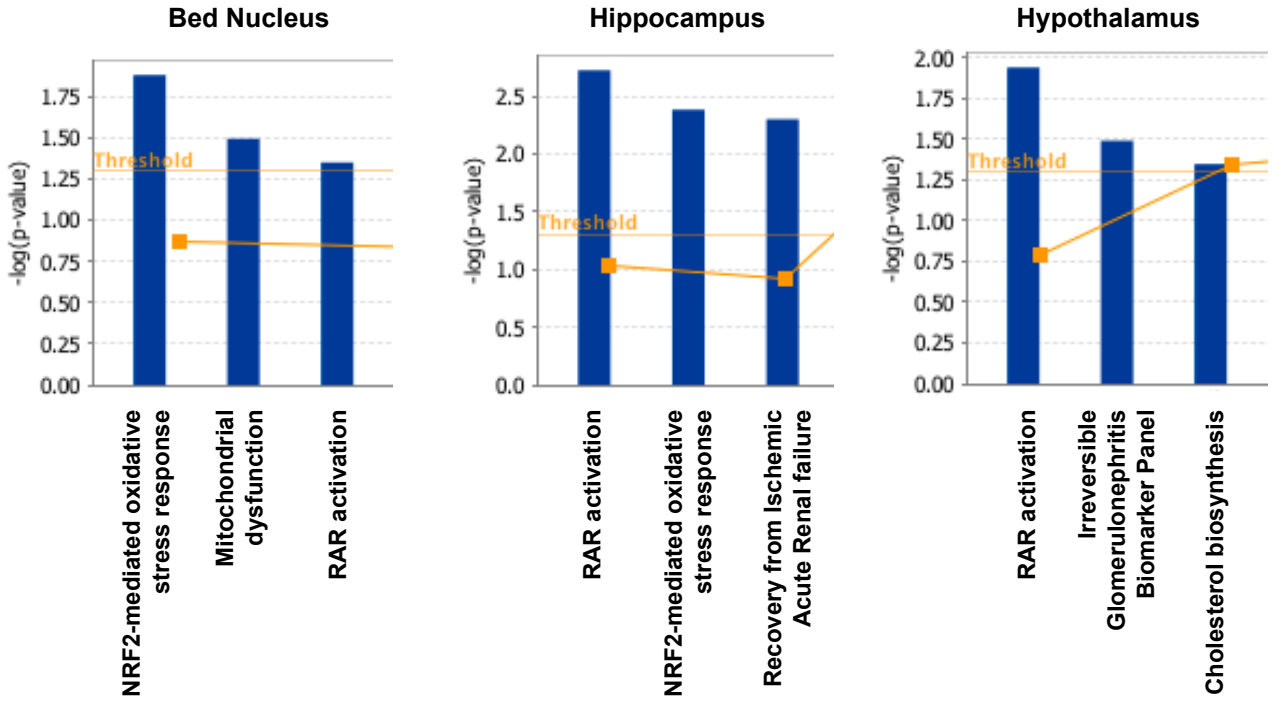

B **Distinct RAR activation in the hypothalamus of C57BL/6 vs FVB mice**

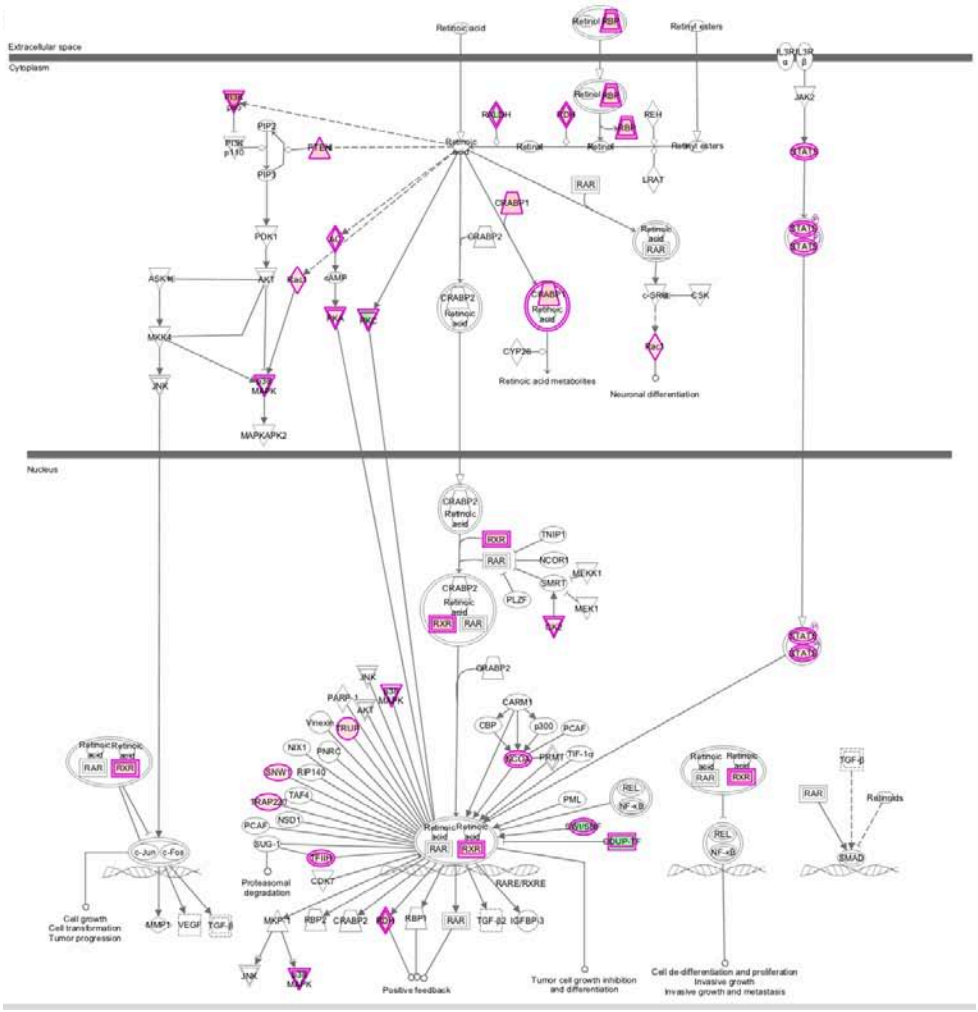

A

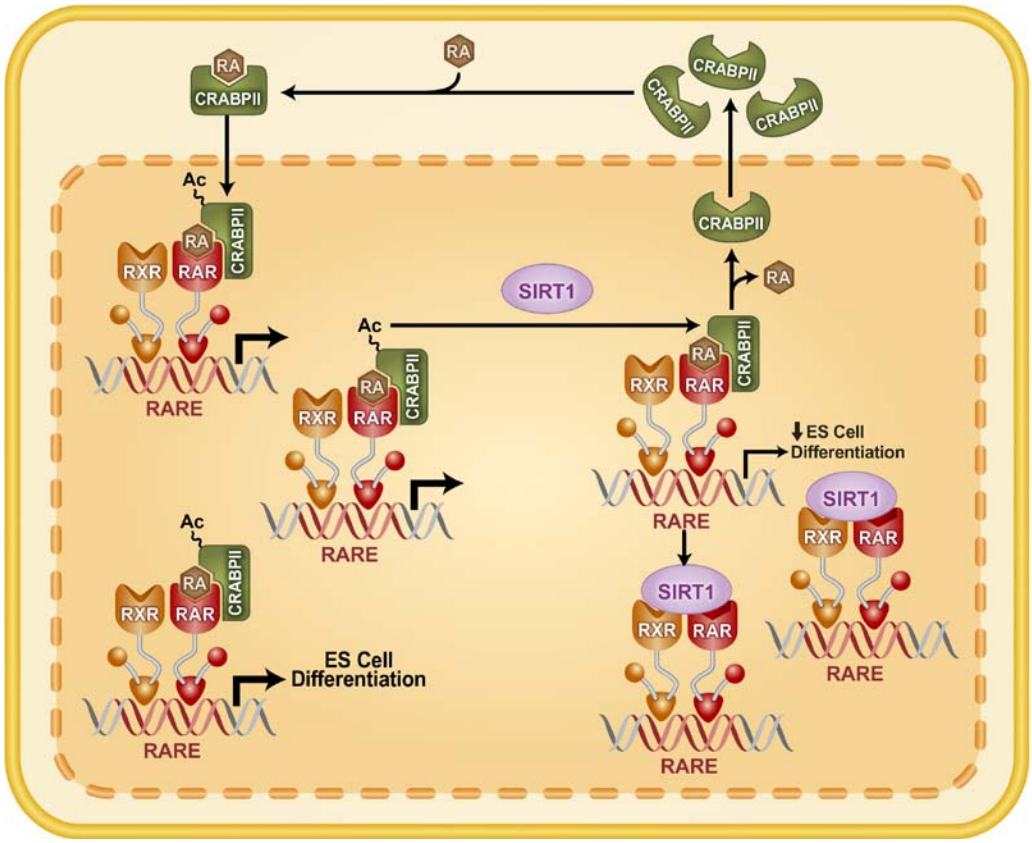
RA
CRABPII
CRABPII
CRABPII
CRABPII
Ac
RA
RXR
RAR
CRABPII
RARE
SIRT1
RA
ES Cell
Differentiation
ES Cell
Differentiation

B

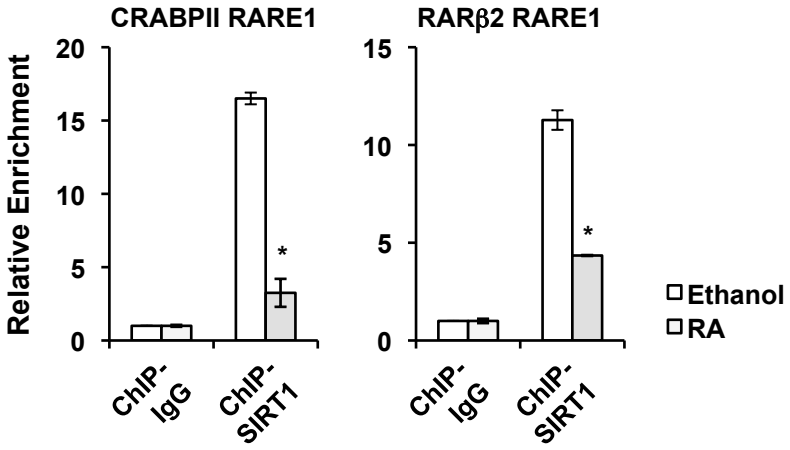
CRABPII RARE1
RARβ2 RARE1
Relative Enrichment
20
15
10
5
0
*
ChIP-IgG
ChIP-SIRT1
Ethanol
RA

Supplementary figure legends

Figure S1. CRABPII K102 is the key residue that affects its RA-induced nuclear translocation. Related to Figure 1 and Figure 2.

(A) CRABPII, but not CRABPI, interacts with SIRT1 in cells.

(B) Quantification of the subcellular localization of WT and mutant CRABPII proteins in WT and SIRT1 KO MEFs. (Left) The subcellular localizations of WT and mutant CRABPII proteins in WT and SIRT1 KO MEFs were analyzed in 60-100 cells, and percentage of cells with different localization of CRABPII was calculated. (Right) The intensity of nuclear CRABPII and cytoplasmic CRABPII were quantified in at least 20 cells as described in the Experimental procedures, and the ratio of Nuclear/Cytoplasmic CRABPII were calculated. *$p<0.05$, values are represented as mean $\pm$ SEM.

(C) K to R mutation of K102 site disrupts RA-induced nuclear translocation of CRABPII. MEFs expressing the indicated CRABPII proteins were treated with 0.1 μM RA for 6 hours. Cells were then fixed and analyzed for subcellular locations of CRABPII.

(D) The expression levels of WT, K102R, and K102Q proteins in stably MEF lines used for Figure 2D and S2B.

Figure S2. SIRT1 deficiency enhances mESC differentiations in response to the RA treatment. Related to Figure 3 and 4.

(A) SIRT1 interacts with CRABPII but not CRABPI in E14 mESCs.

(B) SIRT1 KO mESCs have increased accumulation of CRABPII in the nucleus. The intensity of nuclear CRABPII and cytoplasmic CRABPII were quantified in about 60 cells as described in the Experimental procedures, and the ratio of Nuclear/Cytoplasmic CRABPII were calculated. Histograms were made with SigmaPlot software. * $p<0.05$.

(C) WT and KO mESCs in the ESGRO medium were stained for the AP activities.

(D) Knocking-down SIRT1 induces differentiation of mES cells in the ESGRO medium. Sh-Control and sh-SIRT1 mESCs were stained for the AP activities, and the staining intensity was quantified in 60-100 colonies as described in Methods.

(E) Sh-Control and sh-SIRT1 mESCs were treated with 20 nM of RA in the M10 medium for indicated days.

Figure S3. IPA analyses of transcriptomes of sh-Control and sh-SIRT1 mESCs. Related to Figure 5.

(A) The “Wnt/β-catenin signaling pathway” is upregulated (red) in sh-SIRT1 mESCs.

(B) The “Role of Oct4 in Mammalian Embryonic Stem Cell Pluripotency pathway” is downregulated (green) in sh-SIRT1 mESCs. 1,468 significantly changed gene probes in RA treated sh-SIRT1 and sh-Control samples were analyzed by IPA.

Figure S4. CRABPII expression levels in mESCs transfected with control or CRABPII siRNAs. Related to Figure 6.

(A) Both CRABPII 3'UTR siRNA (siRNA targets 3'UTR of CRABPII gene) and CRABPII siRNA (siRNA targets the protein coding region of CRABPII gene) can efficiently knock down the mRNA levels of endogenous CRABPII.

(B) CRABPII 3' UTR siRNA fails to knock down the mRNA levels of overexpressed WT and mutant CRABPIIs.

(C) The CRABPII K102Q mutant has increased ability to induce mESC differentiation morphologically. mESCs stably expressing indicated CRABPII proteins were cultured in the ESGRO medium. The AP activities were stained and the staining intensity was quantified in 60-100 colonies as described in Methods.

Figure S5. Deletion of SIRT1 in mice leads to developmental abnormalities and abnormal RA signaling in newborn mice. Related to Figure 7.

(A) SIRT1 deficiency on the C57BL/6J background leads to developmental abnormalities. SIRT1 KO embryos (E14.5, E16.5, E18.5) and newborns (P0.5) display growth retardation. Bar, 2 mm.

(B) IgG negative control staining in osteoblasts (left panels) and chondrocytes (right panels). Bar, 10 μm. Vertebral sections from WT and SIRT1 KO newborn pups (P0.5) were stained with normal IgG.

(C) Adult SIRT1 KO mice in a mixed 129SVJ/CD1 background have enhanced expression levels of a number of RA target genes in testis. n=4, *$p<0.05$.

(D) SIRT1 liver-specific KO mice (LKO) have an increased hepatic transcriptional response to the RA treatment compared to control mice. Male Flox and SIRT1 LKO mice were fed with a vitamin A deficient diet for 8 weeks, and then given a dose of 5mg/kg *all-trans* RA via intragastric gavage. Livers were harvested 24 hours later and total mRNA was analyzed by qPCR (n=5, *p<0.05).

Figure S6. Brains from mice on C57BL/6 or FVB background have distinct RA signaling pathways. Related to Figure 7.

(A) Top three differentially expressed canonical pathways in three different regions of mouse brains on the C57BL/6 background compared to the FVB background. Microarray data from GSE3327 dataset were analyzed by IPA.

(B) The “RAR activation pathway” is generally hyper-activated (red) in the hypothalamus of C57BL/6 mice compared to FVB mice. Microarray data from GSE3327 dataset were analyzed by IPA.

Figure S7. SIRT1-mediated deacetylation of CRABPII modulates RA-induced ES cell differentiation. Related to Figure 1 to Figure 6.

(A) A working model for the action of SIRT1/CRABPII in cellular RA signaling and ES cell differentiation. Our data indicate that the acetylation status of K102 of CRABPII protein directly influences its subcellular localization. Acetylation of K102 promotes nuclear accumulation of CRABPII, enhancing its ability to co-activate RAR and promoting ES cell differentiation. SIRT1 deacetlyates

CRABPII, promoting its recycling to the cytosol and subsequent inactivation of RAR, and thereby inhibiting ES cell differentiation.

(B) SIRT1 is depleted from RARE upon RA treatment. WT MEFs were treated with or without 0.1 μM RA for 3 hours. Cells were then crosslinked with 1% paraformaldehype and sonicated. Chromatin-IP were performed with anti-SIRT1 antibody (ChIP-SIRT1) or negative control IgG (ChIP-IgG). The the associated DNA fragments were analyzed by quantivative qPCR using primers flanking indicated RAREs.

Table S1. Both CRABPI and CRABPII are hyperacetylated in SIRT1 KO MEFs. Related to Figure 1.

The acetylation levels of all proteins in WT and SIRT1 KO MEFs were analyzed by a SILAC-based lys-acetylomic method as described in Chen et al (Ref. 28 in the main text).

Table S2. Significantly changed gene probes in RA-treated sh-SIRT1 vs sh-Control mESCs. Related to Figure 5.

Cut off: 1.5 folds, adjust p value <0.05.

Table S3. Top 20 Canonical Pathways enriched in RA treated sh-SIRT1 vs sh-Control mESCs. Related to Figure 5.

Significant changed gene list in Table S2 were analyzed by IPA software.

Table S4. Nenonatal death of SIRT1 KO mice in C57BL/6 background. Related to Figure 7.

Four litters of newborn pups were analyzed for their survival at P0.5.

Supplementary Experimental Procedures

Constructs

HA-tagged mouse CRABPI and CRABPII were cloned into pcDNA 3.0 vector. The constructs expressing substitution deacetylation and acetylation mutants of CRABPII were derived from the pcDNA-HA-CRABPII (WT) construct using a Quick-change site mutagenesis kit (Agilent). Lentiviral constructs expressing WT, K102R, and K102Q HA-CRABPII protein were generated with the pHAGE-puro vector. Control shRNA and SIRT1 shRNA lentiviruses were purchased from the Santa Cruz Biotechology.

Cell culture

HEK293T cells and MEFs isolated from WT or SIRT1 KO mice were maintained in Dulbecco's modified Eagle's medium (DMEM) containing 10% fetal bovine serum (FBS).

E14 mESC line was from ATCC, and WT and SIRT1 KO mESCs have been described (McBurney et al., 2003). All stem cells were maintained in the ESGRO Complete Clonal Grade Medium (ESGRO medium, Millipore). To induce the differentiation of mESCs with RA, mESCs were first cultured on gelatin-coated plates in the M10 medium (DMEM, 10% ES cell FBS, 2 mM L-glutamine,

1 mM sodium pyruvate, 0.1 mM nonessential amino acids, 10 μM 2-mercaptoethanol, and 500 units/ml leukocyte inhibitory factor). sh-Control and sh-SIRT1 mESCs were treated with ethanol or 20 nM RA in the M10 medium for indicated times. WT and SIRT1 KO mESCs were treated with 0.2 μM RA.

Immuno-fluorescence assays

Immuno-fluorescence (IF) assays in MEFs and mouse tissues were preformed as described (Grant et al., 2013; Guo et al., 2010). Antibodies: RARβ (abcam, ab53161); SIRT1 (Cell Signaling, #2028); HA (Santa Cruz biotech, sc-7329). WT and SIRT1 KO MEFs stably expressing HA-CRABPII were treated with ethanol or 0.1 μM RA for 6 hours before analysis. Images were taken by a Zeiss LSM 710 confocal microscope and quantified using ImageJ/SigmaPlot software, and confirmed by MetaMorph Offline Version 7.8.6.0 (Sunnyvale). Briefly, for image analysis of nuclear/cytoplasmic intensity of CRABPII using ImageJ/SigmaPlot, the intensity of CRABPII and DAPI along the maximum cell diameter from at least 20 random selected cells per sample was profiled with ImageJ. The nuclear and cytoplasmic CRABPII intensities were then separated by DAPI defined boundary and quantified in SigmaPlot. For image analysis of nuclear/cytoplasmic intensity of CRABPII using MetaMorph, the blue channel (DAPI staining) was used to create a binary mask which identified the nucleus for other channels. This nuclear mask was then inverted to create a mask for the cytoplasm. The nuclear mask was then applied to the green channel to obtain a measurement of the staining intensity in the nucleus. Subsequently, the

cytoplasm mask was then applied to the green channel and an inclusive threshold of 25-255 applied to obtain the intensity of the cytoplasm.

Immunoprecipitation assay

To investigate the interaction between SIRT1 and HA-CRABP proteins in HEP293T cells, HEK293T cells transfected with indicated expressing constructs were treated with ethanol or 0.02 μM RA for 24 hours, cells were then lyzed in the NP40 buffer (50mM Tris-HCL, pH 8.0, 150mM NaCl, 0.5 % NP40) containing Complete TM protease inhibitors (Roche). The whole-cell extracts were immunoprecipitated with monoclonal anti-HA antibody-conjugated agarose beads (Santa Cruz biotech) at 4°C for 2 hours. Immuno-complexes were eluted with the SDS sample buffer and resolved by SDS–PAGE.

To analyze the interaction between endogenous SIRT1 and HA-CRABPII, WT and SIRT1 KO MEFs stably expressing HA-CRABPII were treated with ethanol or 0.1 μM RA for 6 hours. Cell extracts were then immunoprecipitated by anti-HA Agarose beads, and then immunoblotted using antibodies against SIRT1 (Sigma).

Chromatin immunoprecipitation (ChIP) analysis

Chromatin immunoprecipitation (ChIP) analysis was performed essentially as described by the manufacturer (Millipore) with some modifications. Briefly, WT and SIRT1 KO MEFs were treated with or without 0.1 mM RA for 3 hours. Cells were crosslinked with 1% paraformaldehype and sonicated. Chromatin-IP were

performed with anti-HA antibody (ChIP-CRABPII, Santa Cruz biotech, #sc-805), anti-SIRT1 antibody (ChIP-SIRT1, Cell Signaling #2028) or negative control IgG (ChIP-IgG). The associated DNA fragments were analyzed by quantitative qPCR using primers flanking indicated RAREs. Primer sequences: CRABPII RARE1-F: CCTGTCCTCAGCTCAGTTCC; CRABPII RARE1-R: TCTCATCTAGGTGGCCAAGG; RARβ2 RARE1-F: GGGAGTTTTTAAGCGCTGTG; RARβ2 RARE1-R: AACTTTCGGTGAACCCTTCC.

Protein Acetylation Analysis

The hyper-acetylation sites of endogenous CRABPI and CRABPII proteins in SIRT1 KO MEFs were identified with a SILAC-based lys-acetylomic method (Chen et al., 2012). To analyze the acetylation levels of CRABPII in cells, HEK293T cells transfected with constructs expressing HA-CRABPII or WT or HY mutant of SIRT1, and WT and SIRT1 KO MEFs stably expressing HA-CRABPII, were treated with ethanol or 0.1 μM RA for 6 hours. HA-CRABPII was then immunopurified from cell extracts and the acetylation levels were analyzed with anti-acetyl-lysine polyclonal antibodies (Chemicon). To test whether SIRT1 deacetylates CRABPII *in vitro*, acetylated HA-CRABPII protein was immuno-purified with anti-HA antibodies from TSA treated SIRT1 KO MEFs, then incubated with 2 units of purified recombinant human SIRT1 protein with or without 200 μM NAD^+ or 5 mM Nicotinamide as indicated in the deacetylation

buffer (50 mM Tris-HCl, pH 8.0, 137 mM NaCl, 2.7 mM KCl, 1 mM $MgCl_2$, 1 mg/ml BSA, and 200 nM TSA) for 1 hour at 37 °C.